Energy Efficient Network Architecture for Seismic Data Acquisition via Wireless Geophones

Varun Amar Reddy*, Gordon L. Stüber†
Center for Energy and Geo Processing
School of Electrical & Computer Engineering
Georgia Institute of Technology
Atlanta, GA 30332, USA
*varun.reddy@gatech.edu, †stuber@ece.gatech.edu

Suhail I. Al-Dharrab
Center for Energy and Geo Processing
Electrical Engineering Department
King Fahd University of Petroleum & Minerals
Dhahran 31261, Saudi Arabia
suhaild@kfupm.edu.sa

***Abstract*—Traditional seismic data acquisition systems rely on telemetry cables to conduct oil, gas, and mineral exploration. Although cabled systems provide reliable seismic data transfer, their deployment and maintenance costs are increasing substantially as surveys become larger in scale and densely populated. A novel wireless geophone network architecture is proposed and described in this paper, which makes use of the IEEE 802.11af standard. It operates in the TV White Space, which offers a significantly higher transmission range. A data collection scheme is also proposed and its performance in comparison to the default 802.11 schemes is evaluated on NS-3. The proposed scheme is standards compliant; no changes to the IEEE 802.11af standard are required. The problem of hexagonal clustering for orthogonal deployment of geophones is also considered, and the impact of co-channel interference is analyzed. Furthermore, energy-aware algorithms are analyzed to extend the battery life of the geophones. The proposed scheme outperforms the default standard in terms of both throughput and power consumption, and provides a realistic solution for deploying large-scale wireless geophone networks.**

***Index Terms*—wireless geophones, geophone topology, dense wireless networks, 802.11af, TV White Space, power saving.**

I. Introduction

Oil companies use seismic exploration and monitoring to identify new oil and gas reserves. An energy source (either vibroseis or explosives) generates a variable-frequency wave that propagates into the subsurface layers of the Earth. The reflected waves are detected by geophones, and then transmitted to a data collection center. After collecting and processing the data, a visual image of the Earth's subsurface is obtained.

The topics of 2-D and 3-D seismic survey design and planning have been elucidated in [1], [2]. A typical land seismic survey deployment consists of 10,000 to 30,000 geophones, covering an area of up to 100 km^2. The geophones are positioned along a straight line, 5-30 meters apart, forming the Receiver Line (RL). Large vibroseis trucks move in straight lines, called the Source Lines (SL). The trucks generate seismic waves, termed as a *shot*, for a duration of 4-12 s, known as the *sweep length*. The geophones collect data for a similar duration, known as the *listen interval*. Given a seismic wavefield sampling time of 0.5 ms, a geophone with a 24-bit Analog-to-Digital Converter (ADC) will generate data at a rate of 48 kbps. Three-component (3-C) geophones generate thrice the amount of data, at a rate of 144 kbps.

This work is supported by the Center for Energy and Geo Processing at Georgia Institute of Technology and King Fahd University of Petroleum and Minerals, under grant number GTEC1601.

While cabled systems are reliable and effective, they account for a majority of the equipment weight and cost. A significant amount of time is spent in troubleshooting problems pertaining to the cables and connectors. This work proposes to replace cables with a wireless geophone network, which would eliminate the problems associated with laying cables in undulated terrain. It is more cost-effective, as there is less labour work required. More importantly, there is a far less impact on the environment. Power saving schemes are also presented in this paper, thereby enabling the wireless geophones to operate for longer periods of time.

In [3], Savazzi et al. proposed a hierarchical wireless geophone network architecture and overviewed the application of a mixture of wireless technologies such as ZigBee, Bluetooth, Ultra-Wideband (UWB), WiFi, and WiMAX. In [4], Savazzi et al. described a wireless geophone network based on UWB, along with some elements drawn from the ECMA-368 and IEEE 802.15.4 standards. However, these studies do not provide quantitative results and the proposed approaches may require a large number of gateway devices.

Antennas in wireless geophones are located near the ground, with a height less than 1 m. Larsson et al. in [5] have measured propagation loss at Ultra-High Frequency (UHF), for antenna heights between 0.3 m and 1.5 m. Their results show a good agreement with the Two-Ray RF propagation model.

II. IEEE 802.11af Overview

The TVWS (Television White Space) bands are unallocated frequencies that are otherwise used for digital television broadcast transmissions. The typical TVWS spectrum ranges from 50 MHz to 700 MHz. Owing to lower frequencies, the transmission range is significantly increased compared to the 2.4 GHz ISM band. Seismic surveys for oil and gas exploration are usually carried out in remote locations, where white space channels would be plentiful, hence allowing operation with a large amount of bandwidth. The IEEE 802.11af standard operates in the TVWS bands, in addition to IEEE 802.15.4m, IEEE

802.22, and ECMA-392. Comparatively, the IEEE 802.11af standard is easier to set up, and offers better performance in terms of throughput [6], [7].

A. Architecture

The IEEE 802.11af standard makes use of several components for geolocation and white space information [8].

1) Geolocation Database (GDB): The GDB is a database that maps geographic locations to available channels in the area and fulfills regulatory requirements in the TV spectrum. Stations query the GDB to identify and use permitted channels.

2) Registered Location Secure Server (RLSS): The RLSS acts as a local database that contains the operating parameters for a small number of Basic Service Sets (BSSs).

3) Geolocation Database Dependent (GDD) Entities: The term GDD is used to refer to those components of the architecture that are influenced by the GDB.

4) GDD Enabling Station: This component is equivalent to that of a simple Access Point. It obtains white space information from the GDB or RLSS, and controls the operation of the stations in its BSS accordingly.

5) GDD Dependent Station: A GDD Dependent Station can be recognized as a station that is controlled by the GDD Enabling Station.

B. Physical Layer

The IEEE 802.11af standard is based on the Television Very High Throughput (TVHT) PHY [8]. The possible channel bandwidths are 6, 7, and 8 MHz. Channel bonding can occur between contiguous or non-contiguous channels, each of width W, to yield channel bandwidths of $2W$ or $4W$.

III. Proposed Network Topology and Architecture

As in most analyses of geophone networks, the orthogonal geometry is assumed [1]. In this type of arrangement, the RLs and SLs are perpendicular to one another. Fig. 1 depicts a topology that specifies an inter-geophone distance of 25 m along the RL, and an inter-RL distance of 200 m. There are a total of 30 RLs, each comprising 480 geophones. This amounts to a total of 14,400 geophones, that map an area of approximately 72 km^2. Wireless coverage can be provided throughout the entire area by dividing it into tessellating hexagonal cells. Note that several other possibilities for orthogonal deployment exist; Fig. 1 merely depicts one such case.

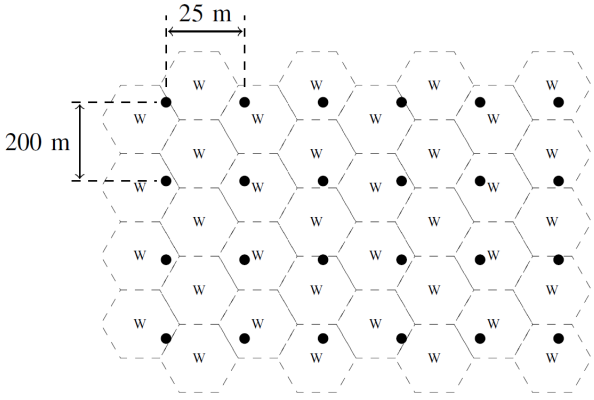

Fig. 1: Orthogonal Deployment of Geophones

Let R be the radius of the hexagonal cells, X be the number of geophones placed in a single RL, Y be the total number of RLs, Δx be the spacing between geophones, and Δy be the spacing between the RLs. The number of cells, *N(R)*, required to map the entire area can then be computed as:

$$N(R) = \begin{cases} (2\lceil y_c \rceil + 1)\lfloor x_c \rfloor + \lceil y_c \rceil & \{x_c\} \leq 1/3 \\ (2\lceil y_c \rceil + 1)\lceil x_c \rceil & \{x_c\} > 1/3 \end{cases} \quad (1)$$

where

$$y_c = \frac{(Y-1)\Delta y}{\sqrt{3}R}, \qquad x_c = \frac{(X-1)\Delta x}{3R},$$

and $\lceil \alpha \rceil$, $\lfloor \alpha \rfloor$, $\{\alpha\}$ denote the ceiling, floor, and fractional part of α respectively. $\lceil y_c \rceil$ denotes the number of cells that would occur in a single vertical 'column' of cells, as illustrated in Fig. 1. Similarly, $2\lceil x_c \rceil$ denotes the number of cells that would occur in a single horizontal 'row' of cells. Note that 2 adjacent cells are contained in a horizontal span of $3R$. The hexagon is an ideal choice for the cell shape, as it closely approximates a circle and provides a range of tessellating frequency reuse cluster sizes [9]. Naturally, the number of available channels would determine the cluster size. A major drawback of using such an approach is co-channel interference, which increases the probability of outage.

Fig. 2 provides an illustration of the proposed architecture based on the IEEE 802.11af standard. Each cell is serviced by a Wireless Gateway Node (WGN) that collects data from all the geophones within the cell area. A star topology is preferable, as the geophones would not have to spend additional energy on relaying information through a multi-hop network. The WGNs can be provided with larger storage and energy capabilities. The collected information is then relayed to the Data Collection Center (DCC), which is supported by a taller antenna. Abiding by the conventions laid out by the IEEE 802.11af standard, the DCC would act as the RLSS, the WGNs would be GDD Enabling Stations, and the geophones would be GDD Dependent Stations.

IV. Proposed GP Scheme

A *Geophone Polling* (GP) scheme is proposed for data collection from the geophones. Its primary features and operation are elucidated below.

A. Key Features

After a shot is fired, the geophones sense the reflected waves for a typical listen interval of 6-12 s. At the end of the listen interval, all the collected data is relayed to the WGN. In the scenario shown in Fig. 2, a single WGN would be overwhelmed by a burst of data from all the geophones. Ideally, the data is successfully transmitted within the sweep length of the next shot, thereby reducing the minimum required storage capacity of the geophones.

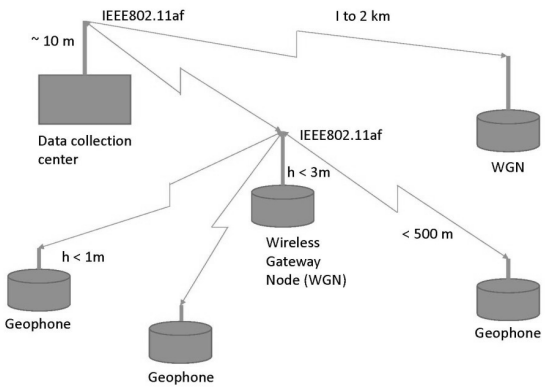

Fig. 2: Proposed Network Architecture

1) Providing Contention-Free Access: The default channel access scheme is provided by the *Distributed Coordination Function* (DCF) [10]. DCF allows stations to access the medium through the Carrier Sense Multiple Access with Collision Avoidance (CSMA-CA) scheme along with binary exponential backoff. At each transmission attempt, the backoff time b depends on the Contention Window (CW) size and the slot time (*aSlotTime*) -

$$b = Rand() \times aSlotTime \tag{2}$$

where Rand() denotes a random integer in the interval [0, CW-1]. The CW size has a maximum value of 1024. For a large number of geophones that are serviced by a single WGN, the CW quickly doubles in size, and the backoff time becomes relatively long. The polling-based scheme that is implemented in the *Point Coordination Function* (PCF) [10], can help reduce the delay associated with large backoff times, by providing contention-free access. The Access Point acts as a Point Coordinator (PC) by designating a Contention Period (CP) where DCF is used, and a Contention-Free Period (CFP) where PCF is used. During the CFP, the PC polls each station with a *CF-POLL* frame, thereby granting it channel access. However, a major drawback in PCF is excessive control signalling. The PC also polls stations that have already transmitted their data, which simply respond with a *CF-ACK* frame. This creates a delay for stations that have data to send and appear much later in the polling list. Let d be the delay associated with the ith station on the polling list, before it can send a data frame.

$$d \geq (i-1) \times [T_{CF-POLL} + T_{CF-ACK}] \tag{3}$$

where $T_{CF-POLL}$ and T_{CF-ACK} denote the time taken to transmit the *CF-POLL* and *CF-ACK* frames respectively. Equation (3) becomes an equality when all the previous $(i-1)$ stations have no data to send. Clearly, for a large number of geophones, the polling list becomes longer and d attains relatively large values. Note that d characterizes the delay associated with just one frame; complete data transfer would involve the transmission of several frames from each station.

The proposed GP scheme mitigates the above problems associated with large values for b and d, by offering each geophone a designated amount of contention-free time with minimal overhead.

2) TCP Fairness: Assuming that TCP is used for data transfer, the problem of TCP fairness is of significant concern in DCF and PCF, as there are several flows sharing the bandwidth [11]. However, in the proposed GP scheme, there is only a single TCP flow, at any point of time.

3) Open Standard: All functionality has been implemented at the application and transport layers. A primary feature of the proposed architecture is to be standards compliant and, hence, the 802.11af PHY/MAC is retained without any changes.

4) Power Saving: The GP scheme conserves power by letting the geophones enter deep-sleep mode (transceiver is switched off) in order to avoid idle listening (listening to the channel when there are no ongoing transmissions) and packet overhearing (listening to ongoing transmissions between other stations). For instance, a geophone can enter deep-sleep after its data has been successfully transmitted.

B. Operation

The proposed GP scheme operates through the services of the DCF, by making use of small User Datagram Protocol (UDP) packets for signalling the individual geophones. A single UDP packet would indicate the start of data transmission from a geophone, unlike the case in PCF, where a *CF-POLL* frame is required for every data frame. The UDP packets do not consume much bandwidth, since the packet size is on the order of a few bytes. They also do not require an acknowledgment from the recipient at the transport layer. Fig. 3 shows the working of the GP scheme.

1) For each shot, the WGN creates a random schedule which determines the order in which the individual geophones will be signalled for data transmission. The schedule is drawn from a uniform distribution, to ensure uniform power consumption for all geophones over several shots.
2) A UDP packet, U_s, is sent to the geophone (G_A) from which the WGN wishes to receive data.
3) Upon receiving U_s, G_A begins to transmit its data, using TCP, to the WGN. When the WGN receives the first data packet from G_A, it stops sending U_s packets to G_A.
4) All other geophones that can hear the RTS/CTS exchange between the WGN and G_A, update their NAV counter accordingly. They enter deep-sleep mode with a sleep duration equal to the NAV duration. This idea has been previously studied in [12], [13].
5) Once data transfer is complete, the WGN closes the TCP connection with G_A. It then sends a U_s packet to the next scheduled station (G_B). Thus, only a single TCP connection is open at any point of time.
6) The WGN also transmits a UDP packet, U_{sl}, to G_A indicating it to enter deep sleep, and to wake up in time for the next shot. G_A responds with a UDP packet, U_{sla}, after which the WGN stops sending U_{sl} packets to G_A.

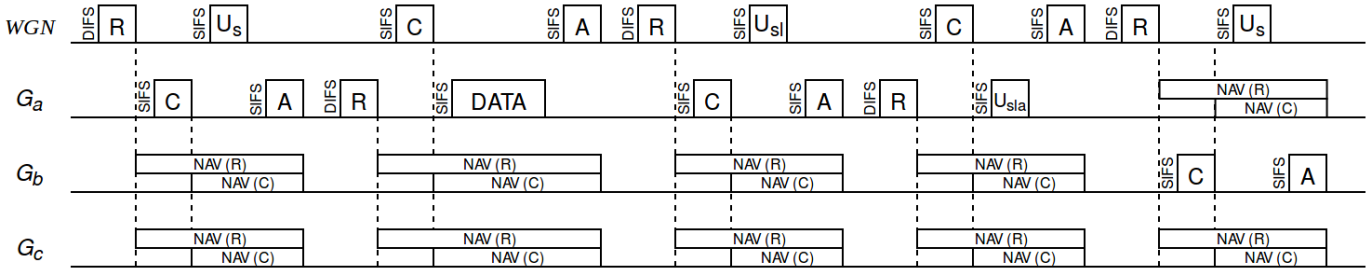

Fig. 3: Working of the Geophone-Polling Scheme (*R*: Request-To-Send, *C*: Clear-To-Send, *NAV*: Network Allocation Vector, *A*: 802.11 Acknowledgement)

7) Steps (2-6) are repeated until data from all the geophones has been received.

V. Performance Evaluation

The performance of the proposed GP scheme is now compared to the DCF and PCF channel access schemes, for a single cell over several shots. The impact of co-channel interference is also analyzed.

A. Simulation Setup

The NS-3 simulator is used for evaluation [14]. The simulation parameters are listed in Table I. An open-area flat-land environment is considered, and the two-ray propagation loss model is used. The short guard interval (2.25 μs for a bandwidth of 8 MHz) is enabled, since the delay spread is typically small in open area environments.

B. Simulation Results

Fig. 4 describes the performance of the GP scheme, in comparison to the DCF and PCF schemes. In Fig. 4a, the time taken by the DCF scheme grows exponentially with an increase in the number of geophones per cell, which is expected. The PCF scheme grows more linearly, but is still inferior to the proposed GP scheme. As the cell radius increases, the polling list becomes larger, and the WGN must poll several 'empty' geophones before interacting with the geophones that have data to transmit. Furthermore, the geophones experience severe contention during the CP. As the cell radius increases, the number of geophones per WGN increases, consequently resulting in reduced throughput, as seen in Fig. 4b.

In Fig. 4c, the power consumption for the GP scheme grows with the cell radius. The last few geophones that are signalled would have to endure a larger number of switches between the transmit and receive states, thereby increasing power consumption. These geophones would also be more susceptible to idle listening and packet overhearing.

TABLE I: Simulation Parameters

Parameter	Value	Parameter	Value
Operating Frequency	470 MHz	Beacon Interval	102.4 ms
Bandwidth	8 MHz	CFP Duration	80 ms
Listen Interval	6 s	SIFS	16 μs
Geophone Data Rate	144 kbps	PIFS	25 μs
WGN Antenna Height	3 m	DIFS	34 μs
Geophone Antenna Height	1 m	RTS/CTS Signalling	Enabled
Max Transmit Power	20 dBm	Short Guard Interval	Enabled
Receiver Sensitivity	-87 dBm	Current (Idle Mode)	273 mA
CCA Sensitivity	-87 dBm	Current (Transmit Mode)	380 mA
Noise Figure	6 dB	Current (Receive Mode)	313 mA
Max PHY Data Rate	35.6 Mbps	Current (Sleep Mode)	33 mA

C. Impact of Co-Channel Interference

An antenna height of 3 m for the WGN creates a severely interference limited system. Suitable antenna heights for the WGN and geophones can be derived, such that the interference power is minimized. For a cell-edge geophone, the following conditions can be imposed:

$$\frac{P_s}{\sum P_{wgn} + \sum P_g} \geq SINR_{min} \quad (4)$$

$$P_s > R_s \quad (5)$$

$$\sum P_{wgn} < CCA_s \quad (6)$$

$$\sum P_g < CCA_s \quad (7)$$

where $SINR_{min}$ is the minimum required SINR for reliable communication, $\sum P_{wgn}$ is the total worst-case interference power from the surrounding WGNs, $\sum P_g$ is the total worst-case interference power from the surrounding geophones, P_s is the signal power from the WGN of interest, R_s is the Receiver Sensitivity, and CCA_s is the Clear Channel Assessment (CCA) sensitivity. Equations (6) and (7) ensure that the contention space for a given cell is not encroached upon by the surrounding interferers.

The GP scheme is evaluated in Fig. 5 in the presence of co-channel interference, for a cluster size of 4, and possible channel bandwidths of 8 MHz (4 available channels) and 16 MHz (8 available channels). In Fig. 5a and 5b, the performance is reduced due to an increased number of collisions and a lower SNR, as compared to having no co-channel interference. In Fig. 5c, the antenna height for the geophones increases considerably when a larger bandwidth is used, but does not vary much for an increase in the geophone data rate. If three-component geophones (data rate of 144 kbps) with a maximum height of 1 m are used with 4 channels, a radius of 400 m can

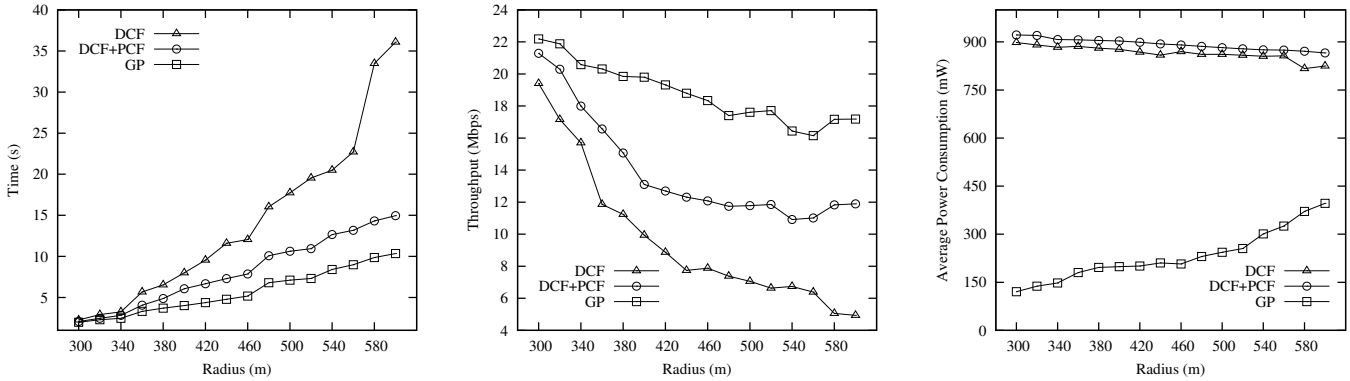

(a) Total Time Taken for Data Transfer (b) Throughput at WGN (c) Average Power Consumption

Fig. 4: Performance Evaluation in terms of Total Time taken, Throughput, and Average Power Consumption

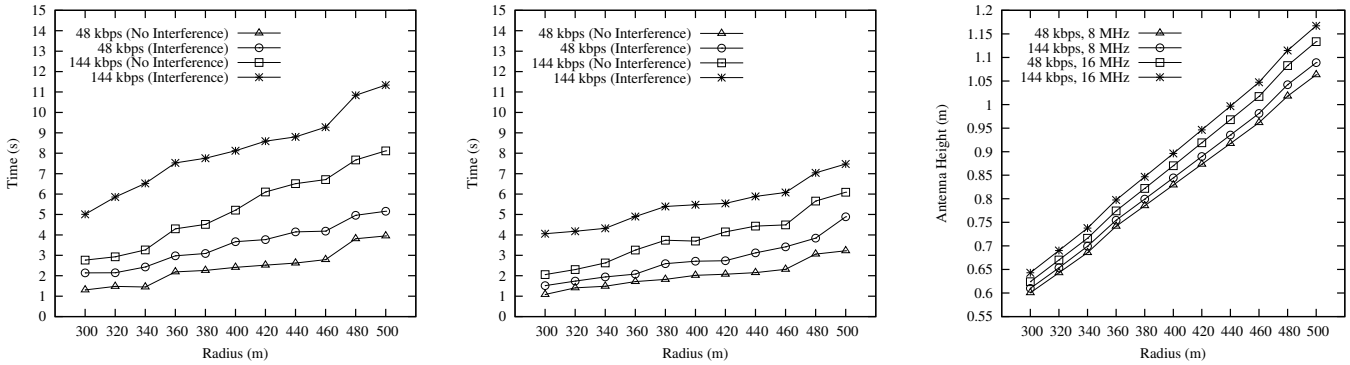

(a) Time Taken for Data Transfer (8 MHz) (b) Time Taken for Data Transfer (16 MHz) (c) Variation of Geophone Antenna Height

Fig. 5: Performance Evaluation in the Presence of Co-Channel Interference

acquire all data in a duration of 8 s. From (1), this amounts to the deployment of around 190 WGNs, for an area of 72 km^2.

VI. Conclusion

In this paper, a wireless geophone network based on the IEEE 802.11af standard is described and evaluated. The proposed GP scheme tackles not only a large area, but also a densely populated network. It performs better in comparison to the default DCF and PCF schemes, by providing contention-free access with minimal overhead. Energy is conserved by putting geophones into deep-sleep mode when they are not operating. Possible geophone network deployments are described, after accounting for co-channel interference. Future work will involve further reduction in energy consumption by relying on the WGN schedule rather than the NAV duration, as a metric for sleep-period determination.

References

[1] G. Vermeer, "3-D Seismic Survey Design," Society of Exploration Geophysicists, 2002.

[2] A. Cordsen, M. Galbraith, and J. Peirce, "Planning Land 3-D Seismic Surveys," Society of Exploration Geophysicists, 2000.

[3] S. Savazzi and U. Spagnolini, "Wireless geophone networks for high-density land acquisition: Technologies and future potential," The Leading Edge, vol. 27, no. 7, pp. 882-886, 2008.

[4] S. Savazzi et al., "Ultra-wide band sensor networks in oil and gas explorations" in IEEE Communications Magazine, vol. 51, no. 4, pp. 150-160, April 2013.

[5] A. Larsson, A. Piotrowski, T. Giles and D. Smart, "Near-earth RF propagation - Path loss and variation with weather," 2013 International Conference on Radar, Adelaide, SA, 2013, pp. 57-63.

[6] J. S. Urn, S. H. Hwang and B. J. Jeong, "A comparison of PHY layer on the Ecma-392 and IEEE 802.11af standards," 2012 7th International ICST Conference on CROWNCOM, Stockholm, 2012, pp. 313-319.

[7] A. Mody and G. Chouinard, "Overview of IEEE 802.22 Standard," June 15, 2010. Available: http://www.ieee802.org/22/Technology/22-10-0073-03-0000-802-22-overview-and-core-technologies.pdf.

[8] A. B. Flores, R. E. Guerra, E. W. Knightly, P. Ecclesine and S. Pandey, "IEEE 802.11af: a standard for TV white space spectrum sharing," in IEEE Communications Magazine, vol. 51, no. 10, pp. 92-100, 2013.

[9] Gordon L. Stüber, "Principles of Mobile Communication (4th ed.)," Springer International Publishing, 2017.

[10] IEEE 802.11: "Part 11: Wireless LAN Medium Access Control (MAC) and Physical Layer (PHY) Specifications," vol., no., pp.1-3534, 2016.

[11] N. Blefari-Melazzi, A. Detti, I. Habib, A. Ordine and S. Salsano, "TCP Fairness Issues in IEEE 802.11 Networks: Problem Analysis and Solutions Based on Rate Control," in IEEE Transactions on Wireless Communications, vol. 6, no. 4, pp. 1346-1355, April 2007.

[12] K. Omori, Y. Tanigawa and H. Tode, "A study on power saving using RTS/CTS handshake and burst transmission in wireless LAN," 2015 10th Asia-Pacific Symposium on Information and Telecommunication Technologies (APSITT), Colombo, 2015, pp. 1-3.

[13] A. Azcorra, I. Ucar, F. Gringoli, A. Banchs, P. Serrano, "μNap: Practical micro-sleeps for 802.11 WLANs," in Computer Communications, Vol. 110, 2017, pp. 175-186.

[14] http://www.nsnam.org/